Estimation of Atmosphere and Object Properties in Hyperspectral Longwave Infrared Data

Jörgen Ahlberg
Swedish Defence Research Agency, FOI
P.O. Box 1165
SE-58111 Linköping
Sweden

jorahl@foi.se

ABSTRACT

We present a method for atmospheric estimation in hyperspectral longwave infrared (LWIR) data. The method also involves the estimation of object parameters (temperature and emissivity) under the restriction that the emissivity is constant for all wavelengths. The method is analyzed with respect to its sensitivity to noise and number of spectral bands. Simulations with synthetic signatures and signatures from real vegetation are performed to validate the analysis.

The proposed method allows estimation with as few as 10–20 spectral bands at moderate noise levels. Using more than 20 bands does not improve the estimates.

1.0 INTRODUCTION

Multi- and hyperspectral image exploitation is a growing field both in remote sensing within the civilian community and in defence applications such as reconnaissance and surveillance. Multi- and hyperspectral electro-optical sensors (cameras) sample the incoming radiation at several (multispectral sensors) or many (hyperspectral sensors) different wavelength bands. Compared to a consumer camera that, typically, uses three wavelength bands, corresponding to the red, green and blue colours, hyperspectral sensors sample the scene at a large number of wavelengths (spectral bands), often several hundred. Moreover, these spectral bands can be beyond the visible range, i.e., in the infrared domain. Each pixel thus forms a vector of measurements from the different bands. This vector, the observed spectral signature, contains information on the material(s) present in the scene, and can be exploited for detection, classification, and recognition.

At some wavelengths, the influence of the atmosphere between the observed object and the sensor is significant, and it is often necessary to perform atmospheric correction before further processing.[1] Effects of the atmosphere are typically known to some degree; there are standard simulation tools that provide good approximations. This paper treats methods for refining these approximations from observed spectral signatures of unknown objects, i.e., in-scene atmospheric estimation.

1.1. Scenario

A quite specific scenario is considered in this paper, which leads to several assumptions in the treated estimation problems. In our scenario, a reconnaissance aircraft equipped with a nadir-looking sensor has passed over an area, and we want to analyze the observed objects on the ground. The flight altitude is approximately one kilometer. Since we know the time, date, and location, we also have a quite good idea of the atmosphere parameters: humidity and temperature profiles, aerosol and carbon dioxide contents can be read from standard atmosphere models and adjusted using local measurements (e.g., the aircraft can measure the air temperature).

Report Documentation Page

Form Approved
OMB No. 0704-0188

1. REPORT DATE	2. REPORT TYPE	3. DATES COVERED
OCT 2009	**N/A**	**-**

4. TITLE AND SUBTITLE	5a. CONTRACT NUMBER
Estimation of Atmosphere and Object Properties in Hyperspectral Longwave Infrared Data	5b. GRANT NUMBER
	5c. PROGRAM ELEMENT NUMBER
6. AUTHOR(S)	5d. PROJECT NUMBER
	5e. TASK NUMBER
	5f. WORK UNIT NUMBER
7. PERFORMING ORGANIZATION NAME(S) AND ADDRESS(ES) **Swedish Defence Research Agency, FOI P.O. Box 1165 SE-58111 Linköping Sweden**	8. PERFORMING ORGANIZATION REPORT NUMBER
9. SPONSORING/MONITORING AGENCY NAME(S) AND ADDRESS(ES)	10. SPONSOR/MONITOR'S ACRONYM(S)
	11. SPONSOR/MONITOR'S REPORT NUMBER(S)

12. DISTRIBUTION/AVAILABILITY STATEMENT
Approved for public release, distribution unlimited

13. SUPPLEMENTARY NOTES
See also ADB381583. RTO-MP-SET-151 Thermal Hyperspectral Imagery (Imagerie hyperspectrale thermique). Meeting Proceedings of Sensors and Electronics Panel (SET) Specialists Meeting held at the Belgian Royal Military Academy, Brussels, Belgium on 26-27 October 2009., The original document contains color images.

14. ABSTRACT
We present a method for atmospheric estimation in hyperspectral longwave infrared (LWIR) data. The method also involves the estimation of object parameters (temperature and emissivity) under the restriction that the emissivity is constant for all wavelengths. The method is analyzed with respect to its sensitivity to noise and number of spectral bands. Simulations with synthetic signatures and signatures from real vegetation are performed to validate the analysis.

15. SUBJECT TERMS

16. SECURITY CLASSIFICATION OF:			17. LIMITATION OF ABSTRACT	18. NUMBER OF PAGES	19a. NAME OF RESPONSIBLE PERSON
a. REPORT	b. ABSTRACT	c. THIS PAGE			
unclassified	**unclassified**	**unclassified**	**SAR**	**14**	

The sensor is a hyperspectral sensor in the longwave infrared (LWIR) domain with around 200 spectral bands in the 7.5–12 μm interval.

The final goal of the problem studied here can be formulated as follows: Given a hyperspectral observation of a scene in the longwave infrared domain, estimate the emissivity spectrum and the temperature of the observed objects. This problem is commonly referred to as temperature-emissivity separation (TES), and we will study a special case where we put heavy restrictions on the emissivity.

A first step in the TES process is to be able to correct for the atmospheric influence on the observation. The immediate goal of this study is therefore to estimate relevant atmosphere parameters. This is however not completely separable from the TES problem, and, in fact, for certain special cases, the TES problem is solved simultaneously. The secondary goal is to establish sensor requirements, i.e., how many spectral bands are needed at what noise level.

1.2. Related work

Despite a large research effort on atmospheric estimation and correction and its impact on detection, there is little work with the same focus as here, i.e., focusing on minimal sensor requirements. Also, the methods in the literature require either high-resolution spectral data, or use spectral features in other wavelengths than the ones we study here.[2, 3]

The most well-known methods for atmospheric correction are probably AAC[4] and ISAC.[5] Extensions include ARTEMISS,[6] where a database of atmospheric transmissions is used and a smooth emissivity spectrum is retrieved. The type of parameterized models for the atmosphere that we use here is also used by Fox et al.[7] and Chandra et al.[8] The impact of atmospheric correction on target detection is studied by Yuen and Bishop.[1]

1.3. Outline

Section 2 explains how we model the observed objects, the atmosphere, and the sensor. In order to adapt the models to observed data, their parameters are estimated using the optimization procedures described in Section 3. These optimization procedures are analyzed with respect to sensitivity in Section 4 and simulations are performed to validate the analysis and to examine the effects of different spectral resolutions in Section 5. Conclusions are drawn in Section 6.

2. MODELLING

In this section, we describe how we model the three important entities present in our scenario: the observed object, the atmosphere, and the sensor. The type of models used is non-controversial, even if other modelling methods exist, for example subspace models[8] and databases.[6]

2.1. Overview

We want to estimate and study the thermal radiance from an object (or from several objects) represented by a vector $\mathbf{L}_o$ or a continuous function $L_o(\lambda)$.

In a laboratory setting, where the sensor is close to the object, the problem would be considerably less complicated. In our scenario, the sensor is airborne around one kilometer above the observed objects, and we thus need to take atmosphere effects into account. We model the atmosphere by a function $A(\cdot)$, and the at-sensor radiance L_s is thus a function $L_s(\lambda) = A(L_o(\lambda))$.

Disregarding any spatial effects, the sensor is modelled as a global scaling factor and as a spectral filter for each spectral band. The spectral filtering is the function that samples a continuous function $L(\lambda)$ and outputs a measurement vector **z**. The sensor is modelled by a function $S(\cdot)$, and our observation vector is modelled by $\mathbf{z} = S(\, L_s(\lambda)\,)$.

Below, some details about sensor, atmosphere, and object models are given.

2.2. Discretization

In practice, we perform all computations on wavelength-discrete vectors. The resolution of these vectors are either determined by the sensor's spectral resolution or by the high-resolution simulations performed by MODTRAN. These simulations give high-resolution transmission/radiance vectors (every inverse centimeter) that for our purposes serve well as (approximately) continuous functions. The blackbody function determining the object radiance can naturally be computed in any resolution.

2.3. Sensor model

Recalling that we do not make any spatial considerations here, the sensor can be modelled purely as a spectral function $S : \mathcal{L}^2 \rightarrow \mathrm{R}^N$. The sensor inputs an observed radiation $L(\lambda)$ (a continuous function of λ) and outputs a discrete vector **y** of N measurements. Each measurement y_n is a sample of $L(\lambda)$, and it is sampled using a response function $R_n(\lambda)$ centered around λ_n. The response function $R_n(\lambda)$ is typically modelled as a Gaussian function with a certain width δ_n. The sampling is thus expressed by a function $P : \mathcal{L}^2 \rightarrow \mathrm{R}^N$ such that $P(\, L(\lambda)\,) = [P_1(\, L(\lambda)\,), \ldots, P_N(\, \mathrm{L}(\lambda)\,)]^T$. Unfortunately, the sensor is not perfectly linear, but we will in the following assume that the sensor is calibrated as to be linear and with a global scaling factor s compensating for variation in gain and flight altitude. Thus, we model the measurements as

$$y_n = S_n(\, L(\lambda)\,) = s \cdot P_n(\, L(\lambda)\,).$$

The discrete sensor function samples high-resolution vectors using the Gaussian spectral filter. Our *discrete sensor* model, is

$$S(\mathbf{L}) = [S_1(\mathbf{L}) \ \ldots \ S_N(\mathbf{L})]^T$$

which we can write in matrix form so that

$$S(\mathbf{L}) = s\ \mathbf{P}\ \mathbf{L}.$$

2.4. Atmosphere model

The atmosphere between the observed object and the sensor influences the observed signature due to transmission, radiance, and spatial distortion (the latter due to turbulence or scattering into the path). Again, disregarding spatial effects, we model the atmosphere as a spectral function $A : \mathcal{L}^2 \rightarrow \mathcal{L}^2$. The atmospheric transmission is modelled as a multiplicative transmission in each wavelength, and since the atmosphere is also a source of radiation in itself, the model of the observation is

$$A(\, L(\lambda)\,) = \tau(\lambda) \cdot L(\lambda) + L^{\uparrow}(\lambda),$$

where $L^{\uparrow}$ is the up-welling path radiance. Note that this model of the atmosphere assumes a homogeneous layer of air between the sensor and the observed object.

The atmosphere is variable in temperature and humidity (the water vapour content), and these parameters influence the atmospheric transmission and radiance. Assuming that the atmospheric transmission $\tau_d(\lambda)$

without water vapour and the transmission of (a certain amount of) water vapour $\tau_v(\lambda)$ are known, we can parameterize the atmospheric transmission as

$$\tau(w,\lambda) = \tau_d(\lambda) \cdot \tau_v(\lambda)^w, \qquad (2)$$

where the *humidity scaling* w is the relative amount of water vapour, i.e., $w = v/v_0$, where v is the actual amount of water vapour and v_0 is the amount of water vapour giving the transmission $\tau_v(\lambda)$.

The atmosphere radiance depends on the atmospheric transmission and the temperature profile $t_a(z)$, i.e., the air temperature at each altitude z. Here, we simplify the temperature profile to a constant ta and thus use a one-layer atmosphere model. The emissivity spectrum of the atmosphere is $c(\lambda) = 1 - \tau(\lambda)$, and the radiance is thus expressed as

$$L^{\uparrow}(w, t_a, \lambda) = (1 - \tau(w,\lambda)) \cdot L_{bb}(t_a, \lambda) \qquad (3)$$

In the discrete case we have $\tau(x) = \mathbf{T}(w)\,\mathbf{x}$, where $\mathbf{T}(w) = \mathrm{diag}(\boldsymbol{\tau}(w))$ is a diagonal matrix with elements $0 \leq \tau_i \leq 1$. $\tau(w, \lambda)$ depends on the parameter w, as described above. The *discrete atmosphere model* is thus

$$A(\mathbf{L}) = \mathbf{T}(w)\,\mathbf{L} + \mathbf{L}^{\uparrow} = \mathbf{T}(w)\,\mathbf{L} + (\mathbf{I} - \mathbf{T}(w))\,\mathbf{L}_{bb}(t_a),$$

where t_a is the temperature of the atmosphere and $L_{bb}(t)$ is the radiation from a blackbody with temperature t. Note that the equality (2) becomes an approximation in the discrete case. As long as w is close to one, the approximation is close to equality.

The atmospheric transmission used in the experiments in this paper is a simulation of the transmission from ground level to one kilometer above, at midday of a Swedish summer's day. From this, the up-welling radiance can be computed according to (3). The down-welling radiance $L^{\downarrow}(\lambda)$ is simulated for the same time.

2.5. Object model

The radiation at the wavelength λ from an object is the sum of the emitted and the reflected radiation. We write this as $L_o(\lambda) = L_s(\lambda) + L_r(\lambda)$. The emitted radiation is characterized by the object's emissivity spectrum $c(\lambda)$ and its temperature to as $L_s(\lambda) = c(\lambda) \cdot L_{bb}(t_o\ , \lambda)$. In the following, we will consider the special case where the observed object is a graybody, i.e., $c(\lambda) = c$ is constant for all wavelengths. The reasons for using this model are simplicity (two parameters only) and that we in a natural environment have a large chance of finding several graybody pixels.

The reflected radiation depends on the incoming radiation $E(\lambda)$ and the emissivity as $L_r(\lambda) = (1 - c)\,E(\lambda) / \pi$. Note that we neglect any directional effects here, i.e., we assume that the incoming radiation and/or the object surface is 100% diffuse.

Returning to our scenario with an airborne, nadir-looking sensor, and also assuming that we have pure pixels, the discrete object radiance model at pixel coordinate $\mathbf{u} = (u,v)$ is

$$\mathbf{L}_o(\mathbf{u}) = c(\mathbf{u})\,\mathbf{L}_{bb}(t_o(\mathbf{u})) + (1 - c(\mathbf{u}))\mathbf{L}^{\downarrow}\ .$$

where $\mathrm{L}^{\downarrow}$ is the down-welling atmosphere radiance.

2.6. Putting it together

Summarizing the models above we can model the observed vector **z** at image coordinate **u** as

$$\mathbf{z} = S(\, A(\, \mathbf{L}_o(\mathbf{u}) \,) \,) = s\, \mathbf{P}\, A(\, \mathbf{L}_o(\mathbf{u}) \,) = \mathrm{s}\, \mathbf{P}\, (\, \mathbf{T}(w)\, \mathbf{L}_o(\mathbf{u}) + (\mathbf{I} - \mathbf{T}(w)\, \mathbf{L}_{bb}(t_a) \,),$$

where

$$\mathbf{T}(w) = \mathrm{diag}(\, \boldsymbol{\tau}_d \,)\, \mathrm{diag}(\, \boldsymbol{\tau}_v^{\,w} \,)$$

and

$$\mathbf{L}_o(\mathbf{u}) = c(\mathbf{u})\, \mathbf{L}_{bb}(t_o(\mathbf{u})) + (1 - c(\mathbf{u}))\, \mathbf{L}^{\downarrow}$$

- $\boldsymbol{\tau}_d$, $\boldsymbol{\tau}_v$, and $\mathbf{L}^{\downarrow}$ are computed using MODTRAN.
- The sensor is characterized by the parameters s, $\{\delta_n\}$, and $\{\lambda_n\}$.
- The atmosphere is parameterized by w and t_a.
- The object radiance is characterized by $c(\mathbf{u})$, $t_o(\mathbf{u})$, and $\mathbf{L}^{\downarrow}$.

Given the parameters $\mathbf{x} = \{s, t_a, w, t_o, c\}$ we have a *generative model* for the observation. Thus, we can write **y** as a function of a parameter vector **x**, i.e., **y**(**x**).

2.7. Noise model

In practice, the measured vector will not equal **y** exactly, since we have noise and model errors. We have model errors since none of the assumptions above are 100% true, and we have noise added by the sensor. We will model the noise as a being zero-mean, white, additive and with a probability distribution function monotonically decreasing with its square, for example the Gaussian distribution. Thus, our measurement will be $\mathbf{z} = \mathbf{y}(\mathbf{x}) + \mathbf{n}$, where $\mathbf{n} \sim N(0,\sigma^2)$.

3. OPTIMIZATION PROCEDURE

Minimizing the residual between an observation and a parameterized object-atmosphere-sensor model is an optimization problem in several variables. The problem is non-linear in some of the parameters and linear in some.

Having a model vector **y** that depends on a parameter vector **x** and a measurement vector **z**, we estimate the parameters by minimizing

$$f(\mathbf{z},\mathbf{x}) = \|\mathbf{k}(\mathbf{z},\mathbf{x})\|^2 = \|\mathbf{z} - \mathbf{y}(\mathbf{x})\|^2$$

with respect to **x**. The objective function f is non-linear and a suitable optimization algorithm should be applied to find the optimal **x**. The problem is simplified by observing that c and s are linear parameters that can be solved for in a linear sub-problem given values on t_o, t_a and w. Depending on our assumption about the object, this is done in slightly different ways. Using our previous assumptions on the noise, we solve in a least-squared sense, and our notation for a constrained linear least-squares problem is to find

$$\min_{\mathbf{x}} \|\mathbf{C}\mathbf{x}_l - \mathbf{d}\|^2$$

constrained by $\mathbf{A}\mathbf{x}_l \leq \mathbf{b}$.

Given some basic knowledge about the world, we can easily set some constraints on $[t_o, t_a, w]$ as well.

3.1. Single pixel case

In the single pixel case we regard each pixel separately (or we have only one observation). The resulting linear sub-problems (i.e., the derivations of **C**, **d**, **A**, and **b**) for several cases are detailed in the report by Ahlberg.[9]

3.2. Multiple pixel case

When we have multiple (M) observations (pixels) from the same scene, the atmosphere parameters do not change much between the pixels, and in many cases also the sensor scaling should be quite constant. Assuming that these parameters really are constant over the scene, we can formulate a joint optimization problem where we estimate emissivities ($c_1, \ldots, c_M$) and object temperatures ($t_o^1, \ldots, t_o^M$) for each pixel but sensor scaling, atmosphere temperature, and humidity scaling only once per scene, i.e.,

$$\arg\min_{\mathbf{X}} \| \mathbf{Z} - \mathbf{Y}(\mathbf{X}) \|^2 .$$

where

$$\mathbf{X} = [t_o^1 \ldots t_o^M \; c_1 \ldots \; c_M \; s \; w \; t_a]$$

$$\mathbf{Z} = [z_1^T \ldots z_M^T]^T$$

$$\mathbf{Y} = [y_1^T \ldots y_M^T]^T$$

The non-linear problem $\min \|\mathbf{Z} - \mathbf{Y}(\mathbf{X}_{nl})\|^2$ is essentially the same as above, however with $M + 2$ parameters, which makes it a computationally heavy problem.

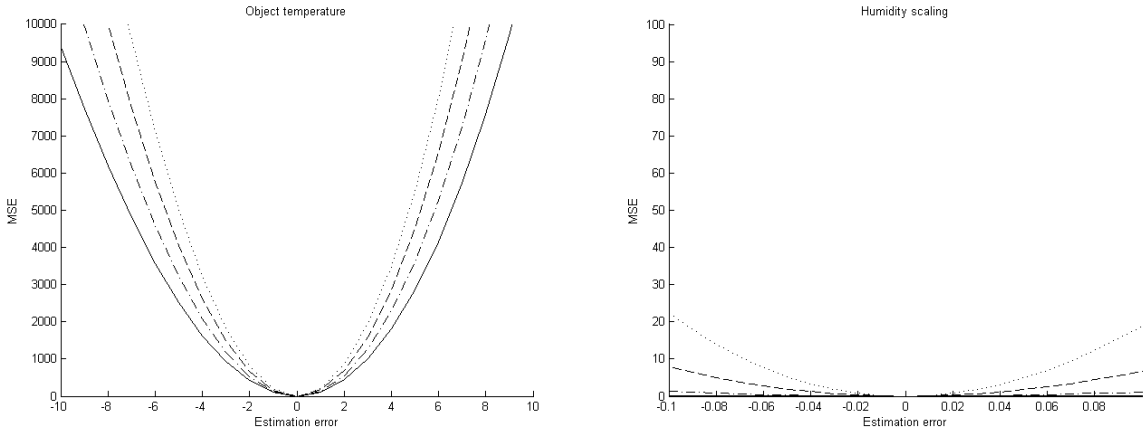

Figure 1. Residuals when perturbing the model parameters from the true values. Left: Object temperature. Right: Humidity. The true parameter values are t_a = 280 K, c = 0.9, s = 1, w = 1. The true object temperature is varied: Solid line: 280 K, dash-dotted: 290 K, dashed: 300 K, dotted: 310 K.

3.3. Large scene case

When the scene is large, it is not feasible to perform the joint estimation using all pixels simultaneously. This is due to two reasons. First, the computational burden will be huge, since the dimensionality of the problem grows linearly with the number of pixels, and the complexity grows exponentially with the dimensionality. Second, the scene might contain many observations of materials that are not graybodies, meaning that the model error will be large.

Although there are several approaches on detecting low-emissivity (near blackbody) objects,[10] the topic is not extensively treated here. Instead, a straight-forward approach is proposed as follows. The input is an initial estimate of the atmosphere's transmission and temperature.

1. Select a random set of observations (K pixels).
2. Perform atmospheric correction of these observations using the initial atmosphere estimates.
3. Fit a graybody curve to each of the corrected observations.
4. Select the observations with small enough fit errors. In practice, this thresholding is relatively simple.
5. Among the remaining observations, select M observations with as different (estimated) temperatures as possible.
6. Use the M selected observations to globally estimate the atmosphere parameters.

Since K is typically much smaller than the number of pixels, this procedure can be run several times to get an estimate of the variance of the parameter estimates.

Evaluation of robust estimation approaches should be done in the future.

4. SENSITIVITY ANALYSIS

The different parameters are not equally prone to estimation errors, and we investigate their sensitivity by generating a model vector $\mathbf{y}(\mathbf{x}_0)$ and then perturbing the parameters one by one, thus generating $\mathbf{y}(\mathbf{x}_{i,j})$ where x_i is perturbed j steps. For each parameter, we compute an error curve e_j telling the mean square error over the residual vector, i.e.,

$$e_j = \| \mathbf{y}(\mathbf{x}_0) - \mathbf{y}(\mathbf{x}_{i,j}) \|^2 / N.$$

We do this for a few different object temperatures, since the sensitivity is highly variable with the object-atmosphere temperature difference. Two of these curves are given in Figure 1, and it is apparent that the object temperature estimation is relatively robust, while the atmosphere humidity scaling is so sensitive that even small amounts of noise will make its estimate almost random. For equal object-atmosphere temperature, it is random even without noise.

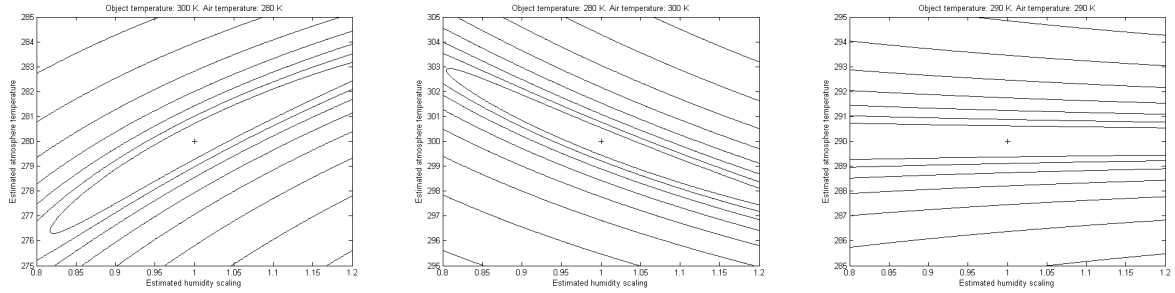

Figure 2. The isocurves of the error at different atmosphere and object temperatures.

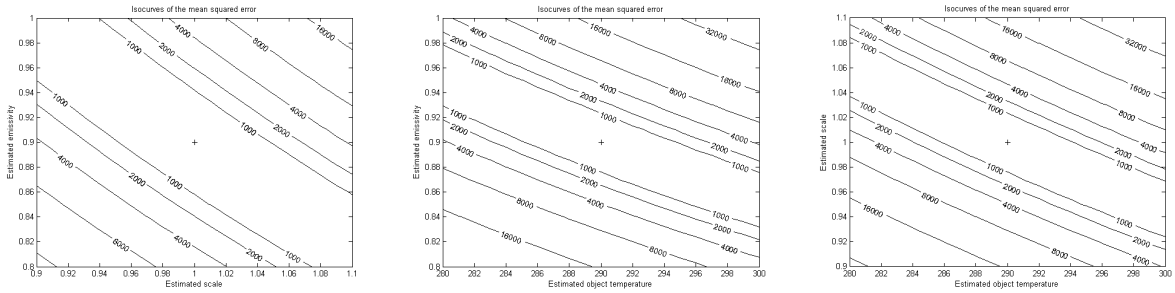

Figure 3. The isocurves of the error when perturbing (pairwise) emissivity, object temperature, and sensor scale.

4.1. Sensitivity of atmosphere parameters

As seen in the previous subsection, the humidity estimate is very error-prone. Note, in particular, the case when the atmosphere has the same temperature as an observed blackbody, i.e., $t_a = t_o$ and $c = 1$. In that case

$$\mathbf{L}_s = \mathbf{T}\,\mathbf{L}_{bb} + (\mathbf{I} - \mathbf{T})\,\mathbf{L}_{bb} = \mathbf{L}_{bb},$$

i.e., $\mathbf{L}_s$ does not anymore depend on the transmission $\mathbf{T}$, and thus not on the humidity w. The humidity estimate will be random.

Instead of plotting the error curve when perturbing the humidity parameter, the error surface when perturbing both atmosphere parameters is illustrated in Figure 2. In the middle graph, the object and atmosphere have equal temperatures, and the error will depend on the atmosphere temperature only. In this case we will still get a relatively robust estimate of the atmosphere temperature. However, for a larger object-temperature difference, we will be able to estimate the humidity, but the estimate is strongly correlated with the atmosphere temperature estimate. That is, an error in the atmosphere temperature estimation can easily be compensated by an error in the humidity scaling estimate. Alternatively, an error in the humidity estimate of 10% will lead to a bias of 2 K in the temperature estimate (this behaviour changes slightly for a graybody).

The conclusions from this are:

- The estimates of all parameters except atmosphere temperature become more robust with a larger object- atmosphere temperature difference.

- Sensor and object parameters are more robust than atmosphere parameters, and the humidity parameter is particularly error prone.
- If one of the atmosphere parameters can be measured accurately in another way, the estimate of the other will be much more reliable.
- If several observations are available, observations with as different object temperatures as possible should be selected.

4.2. Sensitivity of object and sensor parameters

The estimates of atmosphere parameters are virtually uncorrelated with the estimates of the sensor and object parameters. However, the sensor and object parameters are all clearly correlated, as is illustrated by the error surfaces in Figure 3. It is clear that we here have the same problem as mentioned earlier, that an error in one parameter can be compensated with an error in another one. Intuitively, this is expected, since all three parameters c, t_o , and s have the major effect of increasing signal energy at increasing parameter levels.

5. SIMULATIONS

If the observed signal is disturbed by noise, as in all practical cases, the atmospheric estimation and correction is of course degraded. Another factor that influences the quality is the number of bands used. In this section, we simulate a large number of observations in order to see how the performance degrades with increasing noise and fewer spectral bands.

5.1. Test methodology

The parameter estimations have been evaluated by simulations in the following way.

1. Eight different noise levels have been selected, with the variances corresponding to no noise, 0, 20, 40, 50, 60, 70, and 80 dB [μW per sr·cm^2·μm]

2. Atmosphere transmission and sky irradiance were simulated by MODTRAN using models for a Swedish summer's day, as accounted for in Section 2.

3. For each noise level, 200 random spectral signatures have been created in high spectral resolution (one sample per cm^{-1}). The signatures were created by picking the parameters from uniform distributions in the following intervals: $t_o \in [280\ 300]$, $t_o \in [270\ 290]$, $c \in [0.9\ 1.0]$, $w \in [0.9\ 1.1]$, and $s \in [0.9\ 1.1]$.

4. Each of the signatures has been distorted by noise (additive white Gaussian noise).

5. Nine different sensor models have been created, with 3, 5, 7, 9, 12, 15, 20, 30, and 40 spectral bands respectively. The response functions are Gaussians with FWHM = $2 \cdot \Delta\lambda$, where $\Delta\lambda$ is the distance between each band's center wavelength. The band centers are evenly spread out between $8 + \Delta\lambda$ and $11.5 - \Delta\lambda$ μm. Note that the sensors with fewer bands will be less noisy.

6. Each of the sensors sampled each of the $200 \cdot 8$ signatures, and the average absolute errors of the parameters were measured.

This was repeated for four different cases, as described below.

5.2. Simulations using synthetic signatures

We study four different cases, where s and w are known or unknown. From the analysis in the previous section, an unknown humidity is expected to give a larger error in the atmosphere temperature estimate, and an unknown sensor scale is expected to give larger errors in the estimates of the object parameters (t_o and c).

- *Case 1: Known scale and humidity*. In these simulations, *w* and *s* were not randomly picked, but set to a known value (1.0). The results are illustrated in Figure 4 (top row), where the quality (or, rather, the error) of the estimated parameters is plotted against the number of spectral bands for different levels of noise. Two things are clear: (1) When the number of bands is too small, the estimation process is not provided with enough information, and (2) when the amount of noise is too large, the estimation apparently breaks down, and adding more bands does not help. For moderate noise levels (around 20 dB and less), the estimation, as expected, performs better for a larger number of bands. For these noise levels, 9 and 12 bands is enough to get an average error of less than 1 K in the atmosphere and object temperature estimate respectively, and more than 15 bands does not give any significant improvement.
- *Case 2: Known scale, unknown humidity.* In this simulation, *w* was randomly picked but s fixed (and known). The results, see Figure 4 (second row), are not much different from case 1, with the exception of the humidity estimate that is quite bad even for a large number of bands with small amounts of noise (between 0.13 and 0.16 for all noise levels and numbers of bands). The estimate of the atmosphere temperature is worse than for the case with known humidity – around five bands more are required for the same results.
- *Case 3: Unknown scale, known humidity*. In this simulation, *s* was randomly picked and *w* fixed (and known). As expected, the quality of the estimates of the object temperature to is reduced, especially when the number of bands is less than 10.
- *Case 4: Unknown scale and humidity*. In this simulation, *s* and *w* were randomly picked. As expected, the results are approximately the same as in case 3.

5.2.1. Conclusion

The simulations confirm the analysis from the previous section, and also indicate how the estimation quality varies with the number of bands.

- 10 bands or more seem to be needed for accurate estimates.
- Using more than 20 bands does not improve the estimation quality significantly.
- The humidity is hard to estimate, even when using a large number of bands with small noise.
- If the sensor scale is unknown, the estimation quality of the object parameters is reduced.

5.3. Simulations using real signatures

In order to evaluate a more realistic scenario, the simulations above have also been made using real signatures of vegetation. These signatures are laboratory-measured hemispherical reflection of grass, green leaves of birch and aspen, and dry/brown leaves of birch. The leaves are measured on both front and back sides. Instead of randomly choosing an emissivity constant, one of these seven signatures has been selected in the creation of each signature. The results are plotted in Figure 5, and commented as follows:

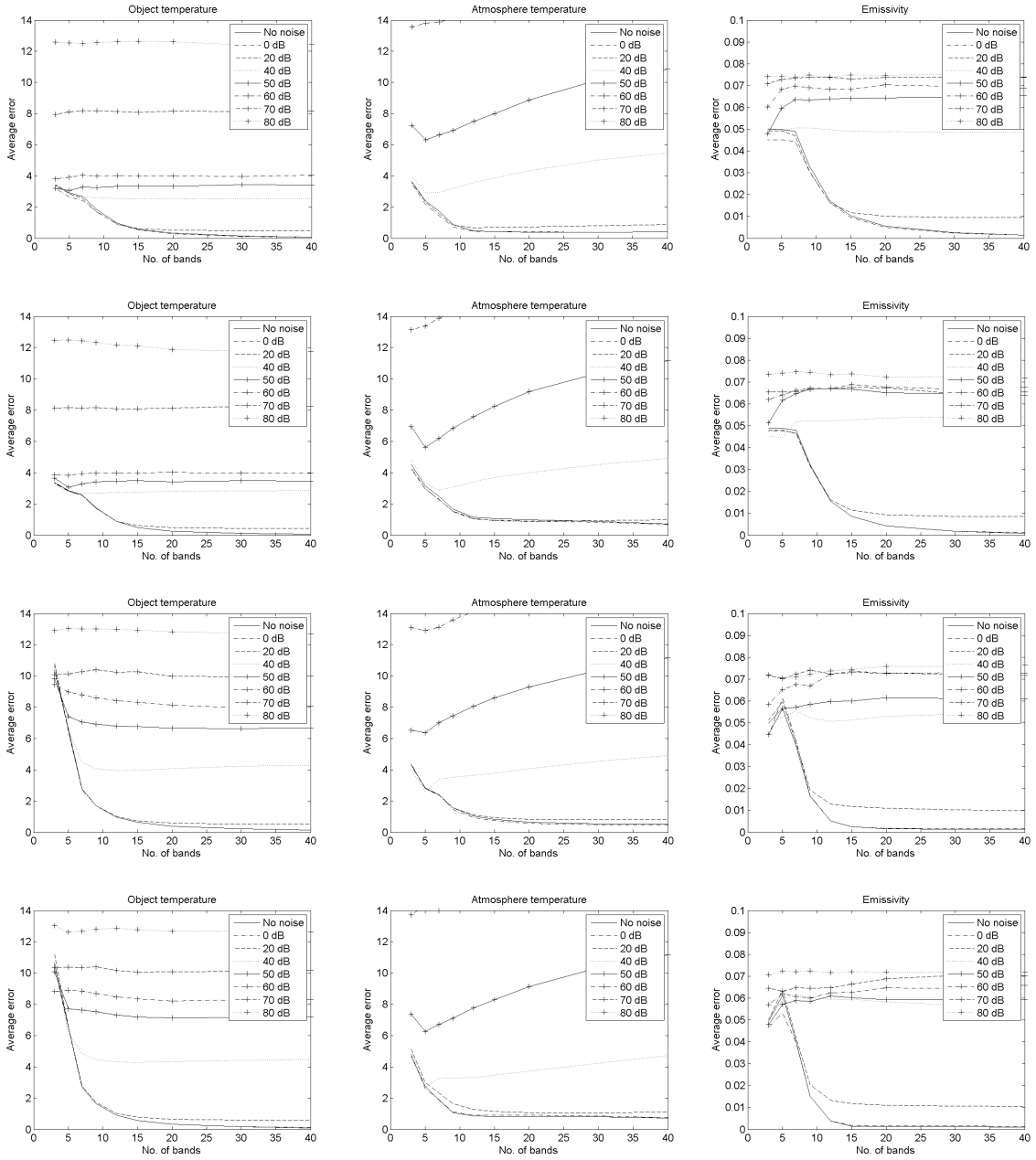

Figure 4. Estimation errors depending on the noise level and the number of bands. The observed objects are graybodies with random emissivities and temperature observed through an atmosphere with random temperature. Top row (case 1): The humidity scaling w and the global scaling factor s are assumed to be exactly known. Second row (case 2): The global scaling factor s is assumed to be exactly known. Third row (case 3): The humidity scaling w is assumed to be exactly known. Fourth row (case 4): Humidity and scaling unknown. In the two latter cases, the signal is scaled with a random scaling factor that is estimated.

- The humidity estimate is, as expected, quite bad (average error of 0.14–0.16 regardless of noise/number of bands).
- The scale estimate is acceptable (average error less than 0.05) for noise levels of 20 dB and less and 10 bands or more.
- The atmosphere temperature estimate is good (average error 2 K or less) as long as the number of bands is more than 5 and the noise is less than 40 dB.
- At a noise level around 50 dB the estimation of atmosphere temperature breaks down, and also gets worse with increasing number of bands.

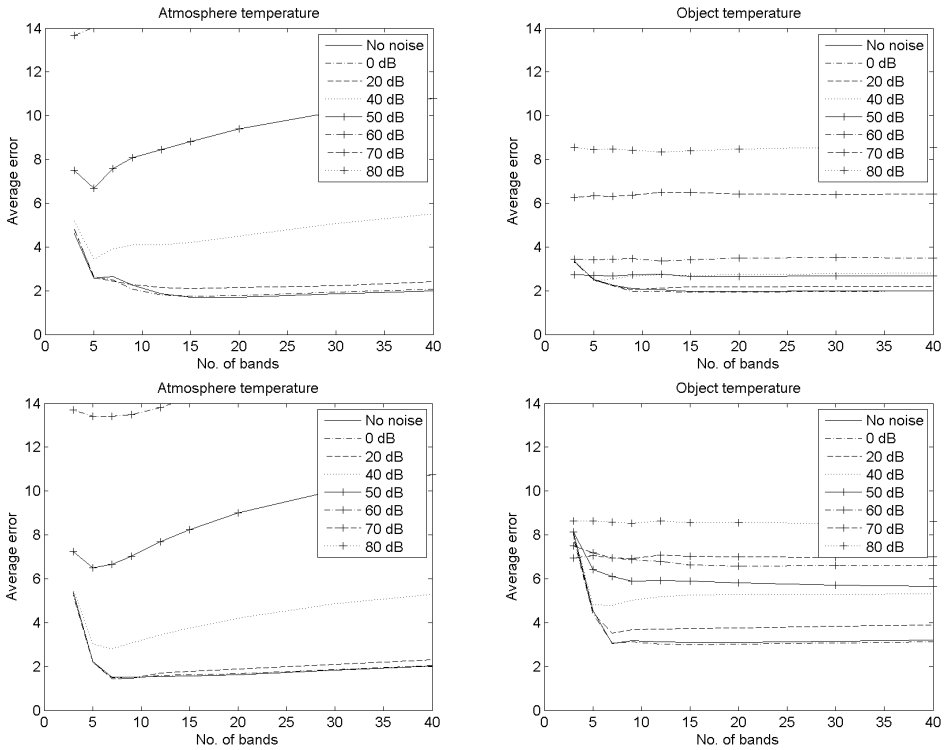

Figure 5. Estimation error as a function of the noise level and the number of bands. The observed objects are randomly selected vegetation components with temperature observed through an atmosphere with random temperature. Top: Humidity and scale are fixed to known values. Bottom: Humidity and scale random (and unknown).

6. CONCLUSION

We have presented a method for atmospheric estimation in hyperspectral LWIR data. The method also involves the estimation of object parameters (temperature and emissivity) under the restriction that the emissivity is constant. The method is analyzed with respect to its sensitivity to noise and number of spectral bands.

In conclusion, the method works well under favourable conditions, but several issues still need to be addressed (as is discussed below). Provided that the noise level is low enough, atmosphere and object temperatures can be estimated with a precision error of around 2 K, using the information from less than 10 spectral bands. If the water vapour content of the atmosphere is unknown and/or the radiometric calibration of the sensor is inaccurate, the precision is of less quality.

ACKNOWLEDGEMENT

This work was funded by the Swedish Armed Forces Research and Development Programme.

REFERENCES

[1] 1. P. W. T. Yuen and G. Bishop, "Enhancements of target detection using atmospheric correction preprocessing techniques in hyperspectral remote sensing," in *Proceedings of SPIE, vol. 5613 (Military Remote Sensing)*, pp. 111–118, 2004.

[2] 2. M. D. Abel, J. M. Zennera, G. A. Petrick, A. T. Buswell, M. L. Pilati, W. R. Czyzewski, L. P. Alessandro, and S. K. Weaver, "A new approach to atmospheric correction of hyperspectral data," in *Proceedings of SPIE, vol. 4725 (Algorithms and Technologies for Multispectral, Hyperspectral, and Ultraspectral Imagery VIII)*, pp. 72–82, 2002.

[3] 3. K. L. Hirsch, L. Balick, C. Borel, and P. McLachlan, "A comparison of four methods for determining precipitable water vapor content from multi-spectral data," in *Proceedings of SPIE, vol. 4381 (Algorithms for Multispectral, Hyperspectral, and Ultraspectral Imagery VII)*, pp. 417–428, 2001.

[4] 4. D. Gu, A. Kahle, and F. D. Palluconi, "Autonomous atmospheric compensation (AAC) of high-resolution hyperspectral thermal infrared remote-sensing imagery," *IEEE Transactions on Geoscience and Remote Sensing*, vol. 38, no. 6, pp. 2557–2570, 1999.

[5] 5. B. R. Johnson and S. J. Young, *In-scene Atmospheric Compensation: Application to SEBASS Data at the ARM Site*,. Aerospace Report No. ATR-99(8407)-1 Parts I and II, 1998.

[6] 6. C. C. Borel, "ARTEMISS – an algorithm to retrieve temperature and emissivity from hyper-spectral thermal image data," in *28th Annual GOMACTech Conference*, Hyperspectral Imaging Session, (Tampa, FL), 2003.

[7] 7. M. Fox, J. Gruninger, J. Lee, A. J. Ratkowski, and M. L. Hoke, "Atmospheric parameterization for model- based thermal infrared atmospheric correction of spectral imagery," in *Proceedings of SPIE, vol. 4816 (Imag- ing Spectrometry VIII)*, pp. 93–103, 2002.

[8] 8. K. Chandra and G. Healey, "Using coupled subspace models for reflectance/illumination separation," in *Proceedings of SPIE, vol. 5425 (Algorithms and Technologies for Multispectral, Hyperspectral, and Ultra- spectral Imagery X)*, pp. 538–548, 2004.

[9] 9. J. Ahlberg, *Estimation of atmosphere and object properties in hyperspectral longwave infrared data*, Scientific report FOI-R--2095--SE, Swedish Defence Research Agency (FOI), October 2006.

[10] 10. R. Kaiser, D. Vititoe, and A. Andrews, "Detecting low-emissivity objects in LWIR hyperspectral data and the corresponding impact on atmospheric correction," in *Proceedings of SPIE, vol. 5093 (Algorithms and Technologies for Multispectral, Hyperspectral, and Ultraspectral Imagery IX)*, pp. 705–718, 2003.